Transport studies in the MAST spherical tokamak

R.J. Akers[1], D.J.Applegate[1], J.Candy[2], G.Colyer[1], D.Dunai[3], A.R. Field[1], W.Guttenfelder[4], J.E.Kinsey[2], M.Reshko[5], C.M. Roach[1], S. Saarelma[1], G.E.Staebler[2], A. Thyagaraja[1], M. Valoviç[1], R.E.Waltz[2], S. Zoletnik[3], O.Zolotukhin[1] and the MAST Team.

[1] Euratom/UKAEA Fusion Association, Culham Science Centre, Abingdon, Oxon OX14 3DB, UK.
[2] General Atomics, P.O.Box 85608, San Diego, California 92186-5608, USA.
[3] KFKI-RMKI, Association EURATOM, P.O.Box 49, H-1525, Budapest, Hungary.
[4] Centre for Fusion, Space & Astrophysics, Dept. of Physics, University of Warwick, Coventry,CV4 7AL.
[5] Department of Physics, University of York, Heslington, York, YO10 5DD, UK.
e-mail contact of main author: rob.akers@ukaea.org.uk

Abstract

Spherical tokamaks (STs) provide a challenging regime for the study of turbulent transport in magnetised plasmas, providing an opportunity to test gyrokinetic and MHD fluid turbulence theory under extreme conditions. The strong field curvature at low aspect ratio has an important influence on micro-stability; both aspect ratio and flow-shear affect transport and at high-β, electromagnetic effects become significant, leading to microtearing instabilities. In this paper, we describe ongoing studies of the dominant transport processes which prevail at low aspect ratio. We present the first non-linear Ion Temperature Gradient (ITG) and Electron Temperature Gradient (ETG) range simulations for MAST using the ORB5 and GYRO models, together with the first results from predictive transport modelling using GLF23 and the next-generation trapped gyro-Landau fluid model TGLF.

1. Introduction

The low moment of inertia of the ST results in strong toroidal rotation, $\omega_\phi \sim 2\times10^5$ rad s^{-1}, driven by the injected torque from the tangentially oriented, mid-plane NBI heating beams, with toroidal Mach number (relative to the thermal deuterium sound speed) between ~0.3 and unity. The E×B flow shear in the core is dominated by the v×B component of the radial electric field, resulting in a marked effect upon transport due to the radial de-correlation of turbulent fluctuations. Discharges heated using counter-NBI injection, for example, benefit from the driven toroidal rotation acting in the same direction as the pressure gradient drive, generating approximately double the E×B shearing rate of co-NBI heated discharges, and on MAST, a significant increase in $H_{IPB98y2}$ (by ~30-40%) [1]. Nonlinear gyro-kinetic simulations indicate that transport in the presence of E×B shear can be modelled via a linear "quench rule", whereby transport is reduced by the factor: $1-\alpha_E\gamma_E/\gamma_{linmax}$, where γ_E is the equilibrium E×B flow shear, $\gamma_{lin,max}$ is the maximum linear growth rate in the absence of flow shear, and α_E~0.5 has been determined from ITG and Trapped Electron Mode (TEM) simulations for conventional aspect ratio and circular flux surface geometry [2]. More recently, nonlinear simulations have extended the quench rule to low aspect-ratio such that $\alpha_E=0.71(\kappa/1.5)/(A/3)^{0.6}$ [3], and so for MAST with A=R/a=1.4 and elongation κ~2.0, α_E~1.5. Thus, full suppression of ITG and TEM turbulence ($k_\perp\rho_i < 1$), favoured by low aspect ratio and the natural high elongation of the ST is predicted to occur when the ExB shear approaches ~70% of the linear growth rate of the most unstable mode in the absence of shear. It is possible to estimate $\gamma_{lin,max}$ analytically for MAST like conditions where the magnetic shear $\hat{s}$ is low [4], and there is negligible interaction between modes on neighbouring rational surfaces. Here, the ITG growth rate is given by:

$$\gamma_{lin,\max}^{ITG} = (\eta_i - 2/3)^{3/4} \, |\hat{s}|^{1/2} \, c_i / |L_S| \qquad (1)$$

where L_s is the magnetic shear scale length, $\eta_i = \partial \ln T_i / \partial \ln n_i$ and $c_i = (T_i / m_i)^{1/2}$. The ExB shearing rate often exceeds $\gamma_{lin,max}$ from eqn. 1 for typical L and H-mode MAST discharges with ion thermal and momentum diffusivity reduced almost to the thermal ion-neoclassical level around the radial zone where ExB shear is maximal [5].

2. Gyrokinetic ITG simulations of MAST

In order to more accurately assess the role of ITG turbulence on MAST, efforts have been directed towards including and bench-marking ExB flow shear in the first-principles based gyrokinetic flux-tube model GS2 [6, 7]. Linear analysis of low in-surface perpendicular wave-number (k_y) mode stability, using GS2 with CYCLONE base-case parameters (with B_T=1.91T, a=0.48m, R_0=1.32m, T_e=T_i) and circular flux surface geometry, reveals a nearly linear dependence on magnetic shear of the value of $\gamma_E/\gamma_{lin,max}$ needed to stabilise the mode, (fig. 1) – at high magnetic shear, resonant flux surfaces are closer together and modes overlap more than at low shear making it more difficult to tear the turbulent eddies apart.

For MAST at mid-radius $\rho_i > 10^{-2}a$, the radial extent of the simulation domain required for nonlinear ITG flux-tube simulations becomes large and the assumption of constant equilibrium quantities and their gradient scale lengths throughout the flux-tube domain breaks down [8]. This problem can be overcome by adopting a "global" approach, whereby profile variation in the simulation domain is modelled. To this end, we have deployed the ORB5 [9,10] PIC (particle-in-cell) gyrokinetic code. The electrostatic ORB5 model solves for the distribution function using the δf method, and for the perturbed electric field using a Poisson solver. A field-aligned filter is applied to the perturbed charge density to suppress noise. Linear ORB5 simulations have been compared with the GS2 flux-tube model for CYCLONE base-case parameters. Scans in ρ^* show agreement between the two models for the maximum linear growth-rate to within ~10% for $\rho^* < 1/50$, with ORB5 showing a rapid fall off at larger values in agreement with linear modelling by Garbet and Waltz [11] and Lin et al. [12]. The width of the steep equilibrium gradient region in ORB5 was found to have only a weak effect on the normalized linear growth rate. Nonlinear source-free ORB5 simulations for CYCLONE base-case parameters allow equilibrium profiles to relax due to the turbulent fluxes until the turbulence becomes suppressed in a quasi steady-state. With adiabatic electrons the nonlinear threshold R_0/L_T (averaged around the steepest gradient region) shows a somewhat flatter dependence on ρ^* above $\rho^* \sim 1/50$ than the linear growth-rate, similar to results obtained using the full-f code GYSELA [13]. ORB5 simulations (using up to 8000 cores on the HECToR supercomputer) find that including trapped electrons kinetically, results in increased ITG turbulence in the nonlinear phase, in line with results from [14].

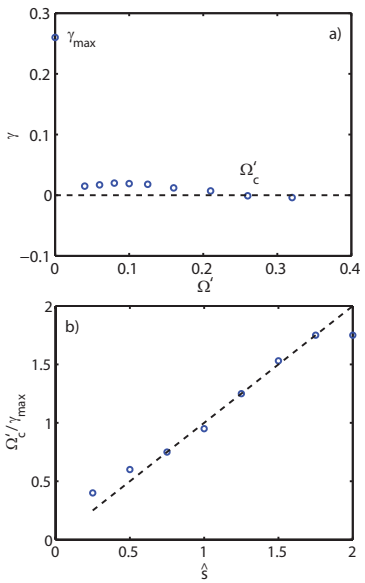

Fig. 1: a) Linear growth rate as a function of rotation shear. Full stability is reached when growth rate becomes zero. b) Critical rotation shear as a function of magnetic shear. $\Omega' = \partial V_{ExB} / dr$ *and* γ *is normalised by* V_{th}/R.

The first source-free ORB5 ITG range, nonlinear global gyrokinetic simulations for MAST conditions have been performed without equilibrium flow shear. Typical L-mode

(#12556 @0.334s) and H-mode (#13018 @0.230s) discharges are deep within the linearly unstable region, with linear modes localized between $0.6< \sqrt{\psi_N} <0.8$ in agreement with earlier flux-tube results where unstable low-k_y modes were identified [15,16]. Nonlinear simulations have been carried out by initializing profiles slightly steeper than the experimental data and letting the turbulence develop and relax the profiles to a quasi steady-state. Nonlinear gyrokinetic PIC simulations are challenging, requiring a large number of particles to reduce the impact of noise (here we have used 67 million markers). Simulations terminate when the initial overshoot in the turbulent flux disappears, and prior to the onset of significant noise (as indicated in fig. 2a) (inset) where the normalized diffusivity is plotted as a function of R_0/L_T. Noise is quantified in ORB5 using the amplitude of perturbed density modes that lie outside the field aligned $k_{||}$ filter. Figs 2a) and 2b) compare the initial and relaxed ORB5 profiles with fits to the experimental data (as deployed in TRANSP). Temperature profiles are found to lie close to the nonlinear threshold (even though simulations omitted sources, trapped electrons and equilibrium flow shear), suggesting that the ITG mode has potentially an important role to play on MAST. A lower temperature gradient was found at mid-radius in L-mode (which may be due to the omission of the ExB flow shear stabilisation). Future work will concentrate on including flow-shear together with sources and a Krook collision operator to reduce the impact of noise as simulations approach steady-state.

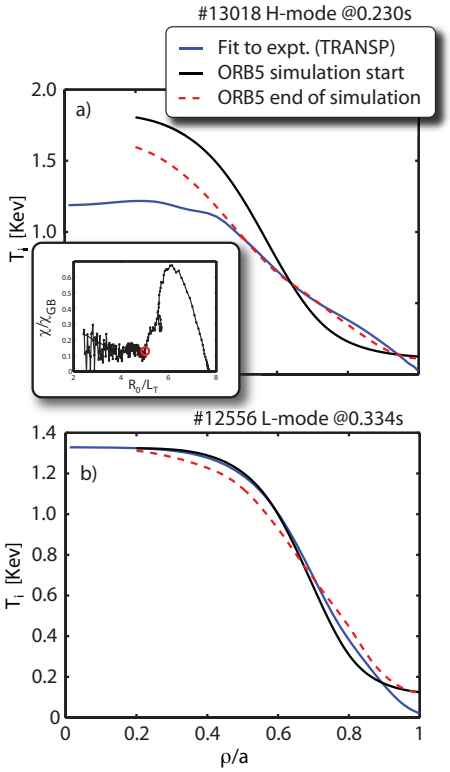

Fig. 2: Experimental data and ORB5 simulation of the ion temperature for H-mode a) and L-mode b) MAST discharges. Inset is the energy diffusivity as a function of critical gradient for the H-mode simulation (which is terminated when noise starts to develop (red circle).

3. Gyrokinetic ETG simulations of MAST

Even when ExB shear should suppress the long wavelength turbulence, electron transport remains well above neoclassical levels (e.g. ion-channel internal transport barriers (ITBs) are seldom accompanied by an ITB in the electron channel). Electron Temperature Gradient ($k_y\rho_i>1$) and microtearing modes are being pursued as potential mechanisms to explain the remaining level of transport.

The linear critical gradient for ETG can be expressed by fitting to a database of gyrokinetic simulations (using the Miller equilibrium model valid for $\varepsilon<0.3$ and low β and ignoring the impact of β' stabilisation) [17]:

$$\left(\frac{R}{L_{Te}}\right)_{crit} = \max\left\{\begin{array}{c}(1+Z_{eff}T_e/T_i).(1.33+1.91\hat{s}/q).(1-1.5\varepsilon).[1+0.3\varepsilon(d\kappa/d\varepsilon)] \\ 0.8R/L_n\end{array}\right\}, \qquad (2)$$

suggesting that many MAST discharges should be ETG unstable for ε~0.3. This expression is being extended to lower aspect ratio and finite β and β′ using GS2 with preliminary simulations based upon CYCLONE parameters (circular flux surfaces, q=1.4, $\hat{s}$=0.8). Fig. 3 shows the variation of critical gradient for two different density gradients and β'=0. Agreement with eqn. 2 is to within 25% for ε<0.4, but with increasing discrepancy towards larger ε.

Nonlinear gyrokinetic ETG simulations with adiabatic ions and zero trapping fraction have previously been shown [18,19,20] to generate experimentally relevant electron thermal transport in conventional tokamak plasmas (e.g. CYCLONE base-case), but with much smaller transport at large positive or negative magnetic shear. Similarly, nonlinear, electromagnetic, GS2 simulations using a numerically calculated equilibrium have demonstrated that ETG transport is experimentally relevant near the mid-radius of an ELMy H-mode MAST discharge [21]. Transport towards the plasma periphery is much smaller, even though the ETG mode there remains linearly unstable. While many parameters are changing across the minor radius, the magnetic shear increases significantly from $\hat{s}$=0.29 to 2.45. Based upon these and other published ETG simulations at varying magnetic shear [20,22], it is likely that the larger magnetic shear plays a significant role in reducing the simulated ETG transport at the edge. We have constructed a phenomenological critical gradient transport model of the form $\chi_e^{ETG} = F(\cdots)(\rho_e^2 v_{Te}/L_{Te})\left[R/L_{Te} - R/L_{Te,crit}\right]$, by estimating the pre-factor F(···), using eqn. 2, from three sets of published simulations where $\hat{s}$ varies from -1.0 to 2.45 [20,21,22]. Fig. 4 shows the inferred value of *F*, peaking for $\hat{s}$~0.8. Far above or below these values the transport is considerably smaller and therefore less relevant experimentally.

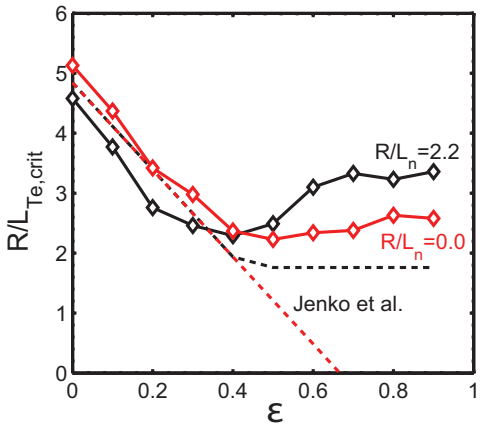

Fig. 3: Variation of critical gradient for two different density gradients and β'=0 (points are GS2, dotted line is a fit by Jenko et al. [17]).

While these independent simulations [20,21,22] demonstrate the generic trend of ETG transport with magnetic shear, they encompass a broad range of parameters: electrostatic and electromagnetic, adiabatic and kinetic ions, zero and finite trapped electrons, s-α and numerical equilibrium. To more systematically quantify the dependence of ETG transport on magnetic shear and *q*, a database of nonlinear electrostatic simulations using GYRO [23] has been created using adiabatic ions and a shaped plasma characteristic of MAST mid-radius using the Miller local equilibrium model (ε=0.3, κ=1.5, triangularity δ=0.2, r/κ·dκ/dr=r·dδ/dr=0.1, dR/dr=-0.25). These calculations include finite E×B shear (γ_E=0.015·v_{Te}/a, characteristic of many MAST discharges), which provides a long wavelength

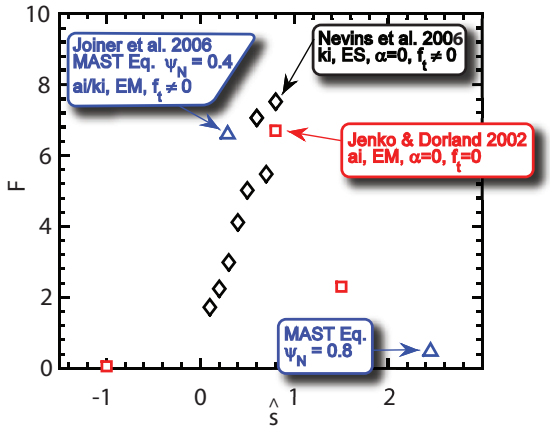

Fig. 4: Pre-factor F(...), encompassing nonlinear influence on ETG transport levels for a number of documented simulations together with MAST simulations

cut-off and physical saturation mechanism for widely varying values of $\hat{s}$ [22,24], but exclude the impact of finite pressure gradient on the equilibrium ($\beta=\nabla\beta=0$). The following grid parameters were used: $L_y \times L_x = 128\rho_e \times 248\rho_e$, $n_y=32$, $n_x=128$, $n_{velocity}=128$. F is found to be sensitive to $\hat{s}$ and q, consistent with previous simulations. In particular, larger transport is recovered as q is increased. Future simulations will include finite beta effects as they are known to impact linear and nonlinear simulations at sufficient values [16].

To compare model ETG transport with radial profiles of experimental transport, the values of F determined from the simulations have been fitted with a simple functional dependence. This parametrization has been used in the critical gradient model together with $R/L_{Te,crit}$ determined from eqn. 2. Additional linear calculations are underway to better characterize the impact of large ε, $\nabla\beta$ and β on the linear threshold value $R/L_{Te,crit}$. Fig. 5 shows model χ_e compared to the experimental χ_e determined from TRANSP for L- (#8505 @0.296s) and H-mode (#8500 @0.295s) discharges. The model predicts experimentally relevant levels of transport near the mid-radius. Towards the edge, where ETG remains unstable, the larger magnetic shear prevents the transport from reaching experimental values. Towards the magnetic axis, ETG is linearly stable. The model χ_e is sensitive to the profiles of q and $\hat{s}$ and will be prone to errors in the equilibrium reconstruction. A new MSE system is being tested in order to accurately determine q and $\hat{s}$ and additional runs with larger box size, increased grid resolution and kinetic ions are underway to test convergence. Although it is not yet clear whether ETG scale turbulence is playing a dominant role on MAST, it is of note that high-k turbulent activity has been identified on NSTX [25].

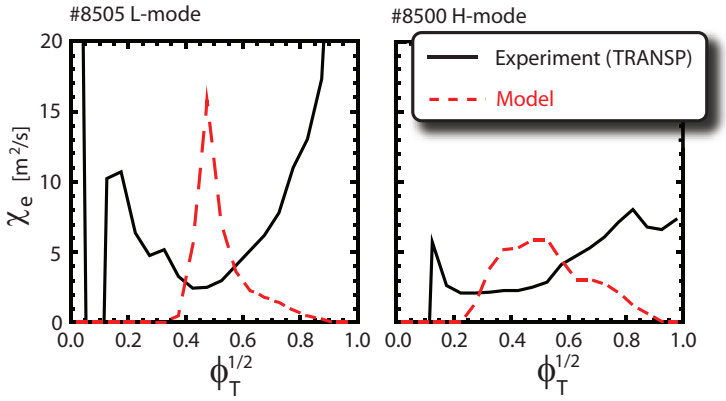

Fig. 5: χ_e from the semi-analytic model based upon non-linear ETG GYRO modelling vs. experiment.

4. Microtearing

GS2 simulations which include electromagnetic effects (including $A_{\|}$ fluctuations) with experimental values of β indicate that microtearing modes are unstable [16], providing another potential candidate for the high levels of anomalous electron transport often observed on MAST. Extensive linear gyrokinetic calculations [26] indicate that the primary microtearing mode drive is through the electron temperature gradient, and that the growth rate is sensitive to magnetic drifts, collisionality and β. These microtearing modes remain unstable with an energy independent collision frequency. An aspect ratio scan indicates that the growth rate reduces only weakly with reducing inverse aspect ratio, and microtearing modes remain unstable for $\varepsilon>0.1$. The local aspect ratio of the ST flux surfaces where microtearing typically arises is close to that in the edge region of conventional tokamaks. A nonlinear model of microtearing turbulence suggests that these modes could be responsible for a substantial fraction of the electron heat flux in the high temperature gradient regions of NSTX plasmas [27]. Preliminary nonlinear microtearing simulations have been performed using GS2 with an approximate s-α model fit to the MAST equilibrium, and tuning some equilibrium parameters to reduce the parallel extent of the modes. Initial calculations for this artificial equilibrium with only four values of k_y, find that after the turbulence starts to saturate, unphysical and rapid growth at the highest radial wave-numbers k_x prohibits further progress in the

calculation. Improvements to the GS2 collision operator [16,26] only postpone the growth at high k_x, which may be due to the accumulation of errors including those from the collision model. Introducing a turbulent hyperviscosity damping term into the gyrokinetic equation suppresses the rapid growth of the high k_x modes, and the hyperviscosity amplitude is found to have no impact upon the linear physics and the turbulence saturation level. On increasing the resolution in k_y to include perpendicular wave-numbers down to $k_y\rho_i \sim 0.1$, a sharp transition to higher magnetic transport was found to be associated with the onset of stochastic magnetic fields (see Fig 6). Such a low k_y on MAST would correspond to n~4, and at low to

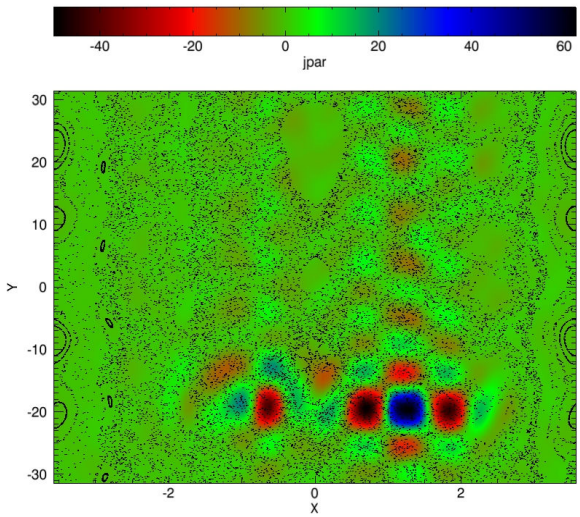

Fig. 6: Microtearing calculation, showing the perturbed parallel current perturbation $J_{||}$ in the plane intersection between outboard mid-plane and the flux-tube (with axes in units of ρ_i). The dots illustrate, via a Poincaré puncture plot, the stochastic perturbed magnetic field.

moderate magnetic shear, the large radial extent of the flux-tube would challenge the validity of the local equilibrium model.

5. Comparison of transport models with experiment

ASTRA [28] and PTRANSP [29] are being used to test transport models for MAST plasmas, including the established dispersion-type drift-wave model GLF23 [30] (which includes Shafranov shift and ExB shear stabilization). ASTRA has been coupled to the NUBEAM [31] gyro-orbit corrected guiding-centre NBI model so as to accurately describe NBI heating and current drive on MAST for the marginally adiabatic orbits [32] resulting from 70keV D injection. L-mode discharge #18696 is sawtooth and tearing-mode free, and exhibits a neutron rate with a temporal evolution accurately modelled by TRANSP (indicating low levels of anomalous fast ion diffusion). Fig.7 shows experimental and model T_e and T_i profiles at various times throughout the discharge (temperature profiles have been set equal to the experimental profiles for r/a>0.8). Typically, the temporal evolution of T_e and T_i (albeit for a limited number of L-mode discharges), demonstrates remarkably good agreement for r/a>0.4, provided ExB flow shear stabilisation is included.

The GLF23 implementation inside ASTRA is currently being benchmarked against PTRANSP, and the transport solvers used by PTRANSP and ASTRA are being compared with XPTOR [33]. These GLF23 simulations nevertheless provide a solid foundation on which to test the next-generation gyro-Landau fluid model TGLF. TGLF improves the accuracy of the trapped particle response and finite Larmor radius effects of the GLF23 model, and includes a new ExB shear quench rule applicable for shaped geometry and low aspect ratio, together with an improved quasi-linear saturation model. First tests of TGLF for

MAST/NSTX conditions have been carried out [34] using an improved neoclassical transport model and an improved collision model. Simulations indicate that ion-thermal transport is close to neoclassical across a large fraction of the plasma (due to ExB flow-shear stabilisation of the ITG mode) in agreement with previous observations/predictions. Improvements to the neoclassical transport model hence proved necessary [35]. Electron thermal transport is predicted by TGLF to be dominated by high-k ETG modes in the mid-radius region of the plasma with some residual trapped electron effects – TEM modes are largely suppressed due to the collisional de-trapping of electrons greatly reducing trapped electron drive in the high collisionality of the low NBI power (<2MW) discharges studied so far. Fig. 8 shows T_e and T_i predicted by TGLF against experiment for MAST H-mode discharge #8500 @0.275s. (MAST #8500 is included in the 2008 public release of the ITPA profile database [36].) Combining this discharge with the other ST plasmas studied in [34], we note that the predicted electron temperature is systematically slightly high, perhaps indicating that the latest collision model is generating too much TEM suppression, that the saturation rule is giving too low a contribution from the high-k modes or that there is some other missing mechanism contributing to the transport (e.g. MHD). It is noteworthy that the experimental core T_e in fig. 8 is lower than the TGLF prediction, similar to many of the GLF23 simulations performed so far. Also shown is the density profile prediction from TGLF for this discharge, the model predicting that hollow profiles, characteristic of typical MAST H-mode discharges are transient (as is known to be the case from 200Hz time resolved Thomson scattering). Further detail concerning tuning and optimisation of the TGLF model to ST conditions is given in [34].

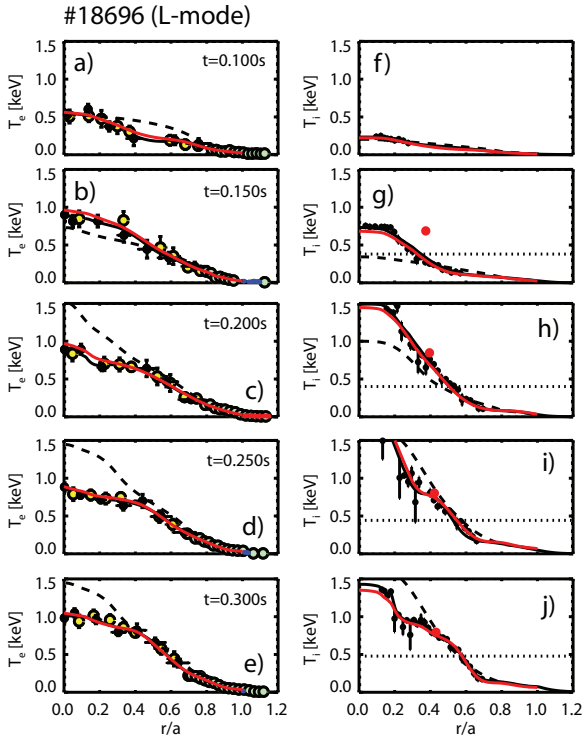

Fig. 7: GLF23 model prediction (dashed) vs. experimental Te (left) and Ti (right) profiles.

6. Summary

Analytic theory, flux-tube gyrokinetic simulations (GS2), and reduced theoretical transport models which deploy a quasi-linear saturation rule (GLF23 and TGLF) all predict that the experimentally observed rotation on MAST should be sufficient to suppress long wavelength turbulence, consistent with observations inferred from experiment (TRANSP) where ion thermal transport is often found to be close to neoclassical. High-k turbulence (ETG) is predicted by TGLF and GYRO (albeit in GYRO without β' stabilisation or large ε effects) to be responsible for at least some of the electron thermal transport outside the plasma core (both codes generating temperature profiles or mid-radius electron thermal transport coefficients close to experiment). Nonlinear GS2 simulations indicate that microtearing may be another possible explanation. Some other, as yet to be determined mechanism (possibly MHD or fast particle driven microtearing) may be necessary to explain core transport where

the temperature gradients are very low (GLF23, TGLF modelling etc. tending to overestimate slightly the core temperatures of MAST plasmas, especially when q_{min}~1). It is interesting to note that the two-fluid MHD turbulence code CUTIE [37] (albeit for circular flux surfaces and zero particle trapping), predicts core temperatures for MAST very close to those observed experimentally. In the plasma periphery, it is possible that long wavelength MHD modes generate significant transport; a prototype beam emission spectroscopy system [38] reveals the presence of relatively high-amplitude density fluctuations (~ few %) in the outer regions of L-mode plasmas with a radial correlation length ~4 cm. In inter-ELM H-mode, coherent MHD activity can be observed in the pedestal region. Future work will concentrate on developing and exploiting the first principles based turbulence codes GS2, ORB5 and GYRO and increasing the number of collisional, nonlinear gyrokinetic simulations used to test and tune the TGLF model. Multi-code benchmarking and testing against experimental data (in particular, taking advantage of a new MSE system and a substantial enhancement of the TS systems on MAST) will assess whether TGLF can be confidently deployed for predicting the performance of future ST devices.

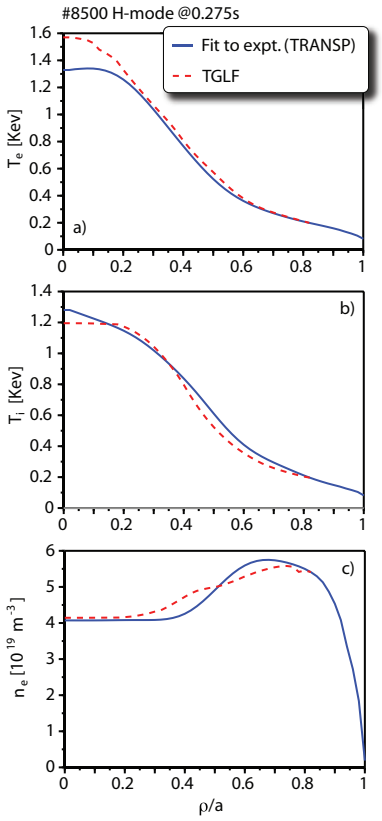

Fig. 8: Experimental temperature and density profiles and TGLF model prediction for H-mode discharge 8500.

References

[1] R. Akers et al., Proc. 21st IAEA Conf., 2006, EX/P3-13
[2] J.E.Kinsey,R.E.Waltz,J.Candy,Phys.Plasmas **12** 062302 (2005)
[3] J.E.Kinsey,R.E.Waltz,J.Candy,Phys.Plasmas **14** 102306 (2007)
[4] A.L.Rogister, Nucl. Fusion **41** 8 (2001) 1101-1106
[5] A.R.Field et al., Proc. 20th IAEA Conf., 2004, EX/P2-11
[6] G.W.Hammet et al., APS-DPP, Philadelphia, Oct 30th 2006
[7] M.Kotschenreuther,G.Rewoldt,W.M.Tang, Comput. Phys. Commun. **88** (1995) 128
[8] S.Saarelma, Joint Varenna-Lausanne International Workshop on Theory of Fusion Plasmas, Aug 25th, 2008
[9] S.Parker, C.Kim and Y.Chen, Phys. Plasmas **6** (1999) 1709
[10] S.Jolliet et al., Comput. Phys. Commun. **177** 5 (2007) 409
[11] X.Garbet, R.E.Waltz, Phys. Plasmas **3** (1996) 1898
[12] Z.Lin et al. Phys. Rev. Letters **88** (2002) 195004
[13] V.Grandgirard et al.,Plasma Phys.Control.Fusion **49** (2007) B173
[14] R.D.Sydora, V.K.Decyk and J.M.Dawson, Plasma Phys. Control. Fusion **38** (1996) A281
[15] D J Applegate et al, Phys. Plasmas 11, 5085 (2004)
[16] C.M.Roach et al., Plasma Phys. Control. Fusion **47** (2005) B323
[17] F.Jenko,W.Dorland,G.W.Hammett, Phys. Plasmas **8** 4096 (2001)
[18] F.Jenko et al., Phys. Plasmas **7** 1904 (2000)
[19] W.Dorland et al., Phys. Rev. Letters **85** 5579 (2000)
[20] F.Jenko and W.Dorland, Phys. Rev. Letters **89** 225001 (2002)
[21] N.Joiner et al., Plasma Phys. Control. Fusion **48** 685 (2006)
[22] W.Nevins et al., Phys. Plasmas **13** 122306 (2006)
[23] J.candy and R.E.Waltz, J. Comput. Phys. 186 545 (2003)
[24] J.candy et al., Plasma Phys. Control. Fusion **49** (2007) 1209
[25] E.Mazzucato et al., Phys. Rev. Letters **101** 075001 (2008)
[26] D.J.Applegate et al., Plasma Phys. Control Fusion **49** (2007) 1113
[27] K.L.Wong et al., Phys. Rev. Letters **99** 135003 (2007)
[28] G.Pereverzev and P.N.Yushmanov, IPP-Report IPP 5/98 February 2002
[29] D.McCune et al., APS-DPP 2007
[30] R. E. Waltz et al., Phys. Plasmas **4** 2482 (1997)
[31] A.Pankin, D.McCune, R.Andre et al. Comput. Phys. Commun. Vol. 159, No. 3 (2004) 157-184
[32] J.Carlsson, Phys. Plasmas, **8** 11 (2001) 4725
[33] J.E.Kinsey, G.M.Staebler and R.E.Waltz, Phys. Plasmas **9** (2002) 1676.
[34] G.E.Staebler et al., Proc. 22nd IAEA Conf., 2008, TH-C.
[35] E.belli & J.candy, Plasma Phys. Contr. Fusion, 50 (2008) 095010
[36] C M Roach et al, to appear in Nuclear Fusion (2008)
[37] A.Thyagaraja, Plasma Phys. Control. Fusion **42** (2000) B255
[38] S.Zoletnik et al., Proc. 22nd IAEA Conf., 2008

This work was funded jointly by the United Kingdom Engineering and Physical Sciences Research Council and by the European Communities under the contract of Association between EURATOM and UKAEA. The views and opinions expressed herein do not necessarily reflect those of the European Commission. We are also grateful to EPSRC for early access to the HECToR supercomputer.